DOI: http://dx.doi.org/10.32571/ijct.515611

E-ISSN:2602-277X

International Journal of Chemistry and Technology

http://dergipark.org.tr/ijct

Research Article

A study on leaching kinetics of chalcopyrite in $KNO_3 + H_2SO_4$ medium

Harun DİKME, Soner KUŞLU*, Özlem KARAGÖZ

ID on the last page

Department of Chemical Engineering, Faculty of Engineering, Atatürk University, 25240, Erzurum, Turkey

Received: 21 January 2019; Revised: 15 April 2019; Accepted: 20 April 2019

*****Corresponding author e-mail: ksoner90@hotmail.com

Citation: Dikme, H.; Kuşlu, S.; Karagöz, Ö. *Int. J. Chem. Technol.* **2019**, 3 (1), 38-45.

ABSTRACT

This paper describes the leaching behaviour and dissolution kinetics of chalcopyrite wıth potassium nitrate in sulphuric acid solutions. Reaction temperature, solid/liquid ratio, stirring speed, chalcopyrite particle size, concentration of sulphuric acid and concentration of potassium nitrate solutions were selected as process parameters. The experimental results were successfully correlated with linear regression using the Statistical package program and dissolution curves were evaluated by the shrinking core models for solid-fluid systems. Finally, it was found that increasing reaction temperature and decreasing solid/liquid ratio caused an increase in the dissolution rate of chalcopyrite. The dissolution extent slightly increased with the increase in the stirring speed rate between 300-900 rpm under the experimental conditions. The activation energy was found as 78.25 kJ mol^{-1}. It was seen that the leaching of chalcopyrite was controlled by surface chemical reactions.

Keywords: Chalcopyrite, KNO_3, leaching kinetics, shrinking core model.

Kalkopiritin $KNO_3 + H_2SO_4$ ortamındaki liçing kinetiği üzerine bir çalışma

ÖZ

Bu makale kalkopiritin sülfürik asit çözeltilerinde potasyum nitrat ile liçing davranışını ve çözünme kinetiğini açıklanmaktadır. Reaksiyon sıcaklığı, katı/sıvı oranı, karıştırma hızı, kalkopirit partikül büyüklüğü, sülfürik asit konsantrasyonu ve potasyum nitrat çözelti konsantrasyonları proses parametreleri olarak seçildi. Deney sonuçları, istatistiksel paket programı kullanılarak lineer regresyon ile başarılı bir şekilde ilişkilendirildi ve çözülme eğrileri, katı-akışkan sistemler için büzüşen çekirdek modelleri ile değerlendirildi. Son olarak, artan reaksiyon sıcaklığının ve azalan katı/sıvı oranının, kalkopiritin çözünme hızında bir artışa neden olduğu bulunmuştur. Çözünme derecesi, deneysel koşullarda 300-900 rpm arasındaki karıştırma hızındaki artışla biraz artmıştır. Aktivasyon enerjisi 78.25 kJ mol^{-1} olarak bulunmuştur. Kalkopiritin liçinginin, yüzey kimyasal reaksiyonlarıyla kontrol edildiği görülmüştür.

Anahtar Kelimeler: Kalkopirit, KNO_3, liçing kinetiği, büzülen nüve modeli.

1. INTRODUCTION

One of the most common minerals in the nature is the compound of sulphur including iron and copper, called chalcopyrite (expressed as $CuFeS_2$ or $Cu_2S.Fe_2S_3$). The use of copper in human history is based on ancient times. Nowadays, even though different metals are used instead of copper in some areas, copper has always kept its importance thanks to its unique properties. High electrical and thermal conductivity, resistance to corrosion and easy processability are some of the important features of copper.

Copper production in the world is carried out by extraction, enrichment and evaluation of copper ores with sulfur and oxides. In general, about 80% of copper production is carried out by pyrometallurgical methods, and hydrometallurgical methods are used at about 20%. Due to the environmental impact, the hydrometallurgical process is becoming an increasing importance. The hydrometallurgical process provides an effective method for processing low-grade ores.[1] The fact that the oxidized sources are preferred more over time, the required chemical materials are with easy and cheap prices, the production facilities can be easily installed where the ore is located, and the low pre-investments and the relatively less damage to the environment increase the popularity of the hydrometallurgical method. For this reason, hydrometallurgical processes are preferred generally for copper extraction. One of the most common minerals in the nature is the compound of sulphur including iron and copper, which is called chalcopyrite (expressed as $CuFeS_2$ or $Cu_2S.Fe_2S_3$). Other than the ore veins, it also occurs typically in low copper concentrates. It is a highly refractory material during the hydrometallurgical process.[2]

Several researchers have reported chalcopyrite leaching. The leaching of chalcopyrite using different leaching solutions has been studied by some investigators (Table 1).

Table 1. Some of the studies aimed at leaching of chalcopyrite in different environments examined by various researchers

Environment	**Activation energy (kJ mol^{-1})**	**Controlling step**	**Ref.**
Water saturated with chlorine	9.06	Controlled by diffusion through the product layer	21
Potassium dichromate	48-54	Chemically controlled	22
By hydrogen peroxide in sulphuric acid	60	The surface reaction controlled	23
In hypochlorite	19.88	By diffusion through the product layer	24
Ferric chloride	68	Chemical reaction	25
Sodium nitrate in sulphuric acid	83	Mixed control	26
Sodium chlorate in hydrochloric acid	60.0 at 298-318 K 57.7 at 318-338 K	By chemical reaction	27

In the hydrometallurgical process, inorganic acids are used as leaching accents.[3] This study aims to investigate the kinetic results for leaching and dissolution processes of chalcopyrite with KNO_3 in H_2SO_4 using a mechanical agitation system. The reaction rates for chalcopyrite are very critical for commercial initiatives. Heterogeneous reaction models were used in the analysis of kinetics for dissolution. In the study, reaction temperature, solid/liquid ratio, stirring speed, chalcopyrite particle size, concentration of sulphuric acid and concentrations of potassium nitrate solutions are used as evaluation criteria for leaching process.

2. MATERIALS AND METHODS

2.1. Materials

The chalcopyrite samples obtained from Artvin Murgul Copper Company were first disintegrated. It was then dried under a vacuum and separated into particle sizes using ASTM standard sieves to give fractions of average dimensions of sizes -50+70, -70+100, -100+120 and -120+140 µm. The chemical analysis of the samples can be seen in Table 2.

Table 2. Chemical analysis of chalcopyrite minerals.

Component	%
Cu	6.70
Ni	0.10
Zn	0.20
SiO_2	45.60
MgO	1.32
CaO	0.28
Fe	18.45
S	19.25
Au	-
Ag	0.0213

2.2. Methods

Atmospheric weather conditions were used to perform the leaching experiments. In the experiments, 500 mL volume global glass reactor was used. A constant temperature water circulation device was used to prevent the temperature change during the experiment. A backflow concentrator was used to prevent evaporation. A mechanical mixer was used to obtain a homogenous mixture. The mechanical agitation test system is quite common and it can be seen in Figure 1. Chemical analysis of chalcopyrite with a particle size of -120 + 140 mesh was performed. Each analysis was repeated twice and the mean values were used in kinetic calculations. The EDS graph of the original mineral is given in Figure 2. Cu, Ni, Au, Ag, Fe and Zn analyses were performed using atomic absorption spectrophotometry (Shimadzu AAS-670). SiO_2 and S analyses were done by gravimetric methods. MgO and CaO analyses were completed with complexometric methods with EDTA.

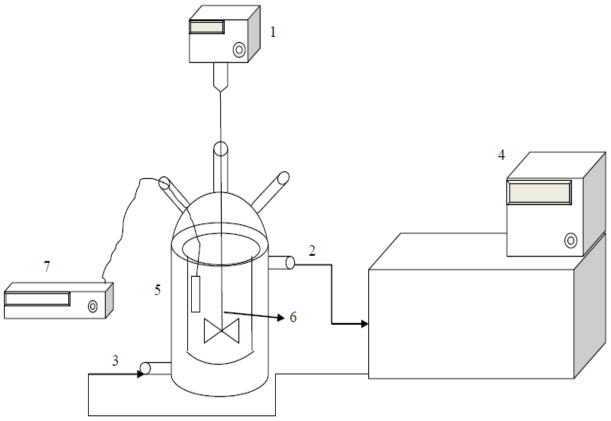

Figure 1. Mechanical Agitation Experimental System. (1. Mechanical agitator, 2. Water output, 3. Water input, 4. Water circulator heater, 5. Glass reactor, 6. stirrer, 7. pH meter).

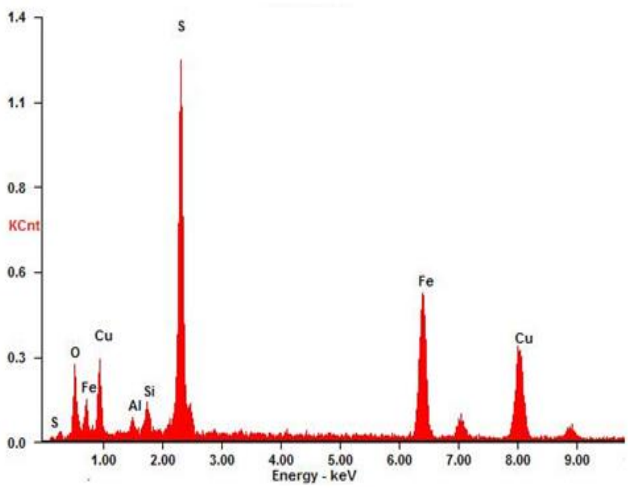

Figure 2. EDS graph of the sample.

3. RESULTS AND DISCUSSION

3.1. Dissolution reactions

Reactions occurring in the reactor can be given as follows.[4-5]

When KNO_3 was used with H_2SO_4, the following reactions occur.

$$H_2SO_{4(aq)} \rightarrow 2H^+_{(aq)} + SO_4^{-2}{}_{(aq)} \qquad (1)$$

$$KNO_{3(aq)} \rightarrow K^+_{(aq)} + NO_3^-{}_{(aq)} \qquad (2)$$

When chalcopyrite is added to the potassium nitrate solution in the reactor, the reaction can be written as follows:

$$CuFeS_{2(s)} + 4H^+_{(aq)} + NO_3^-{}_{(aq)} \rightarrow Cu^{+2}_{(aq)} + Fe^{+3}_{(aq)} + 2S_{(s)} + NO_{(g)} + 2H_2O_{(l)} \qquad (3)$$

The total reaction is as follows:

$$6CuFeS_{2(s)} + 10\,KNO_{3(aq)} + 20H_2SO_{4(aq)} \rightarrow 6CuSO_{4(aq)} + 3Fe_2(SO_4)_{3(aq)} + 5K_2SO_{4(aq)} + 20H_2O_{(l)} + 10NO_{(g)} + 12S_{(s)} \qquad (4)$$

3.2. Effects of parameters

Reaction temperature, solid/liquid ratio, stirring speed, the particle size of chalcopyrite, the concentration of sulphuric acid and the concentration of potassium nitrate solutions were selected as process parameters to measure the effect of chalcopyrite on the dissolution level. Parameter ranges are given in Table 3.

In the experiments, the values of the other parameters were kept constant while the effect of a parameter was examined (see Table 3).

Table 3. Selected parameters and their ranges

Parameter	Values
Temperature (K)	343, 348, 353*, 358
Solid/liquid (g cm^{-3})	1/100*, 1/50, 1/25, 1/10
Stirring speed (rpm)	300, 500*, 700, 900
Particle size (µm)	256, 181, 137.5*, 115.5
Concentration of H_2SO_4(mol dm^{-3})	2.0*, 3.0, 4.0, 5.0
Concentration of KNO_3 (mol dm^{-3})	1.0, 2.0, 3.0*, 4.0

250 mL of KNO_3 solution was used for any trial in the study. The stirrer had a constant velocity of 500 rpm to produce homogeneous concentrations in the batch reactor. Change graphs between time (t) and conversion values (X) are plotted for each parameter. These change graphs can be seen in Figure 3-8.

A 250 mL solution of potassium nitrate was used for all the experiments. The uniformity of the suspension was obtained at a stirring speed of 500 rpm. Therefore, the mixing speed of 500 rpm was a constant value in all experiments to ensure uniformity in the reactor. The plots of time (t) against conversion (X) were obtained.

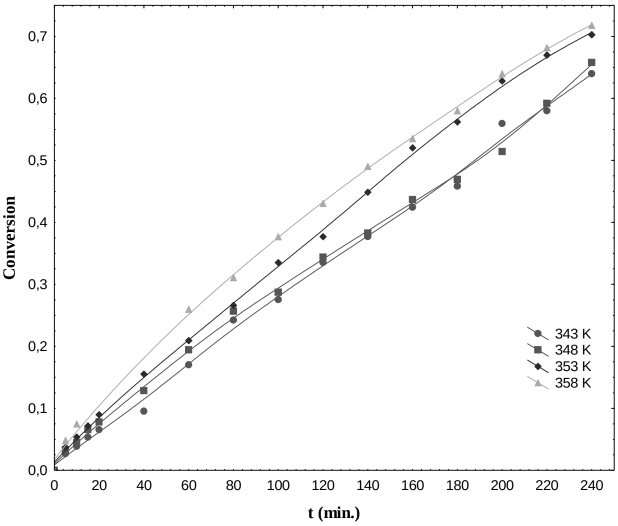

Figure 3. Change graph between time and conversion for different temperatures.

3.2.1. Effect of reaction temperature

There is a significant relationship between the reaction temperature and the speed of the leaching reaction. The experiments were performed at four different temperatures of 343, 348, 353 and 358 K. The curves were plotted as presented in Figure 3.

DOI: http://dx.doi.org/10.32571/ijct.515611 **E-ISSN:2602-277X**

It is seen that the dissolution at higher temperatures is more effective in removing a greater amount of chalcopyrite.[6] The quick production of activation energy helps to accelerate the reaction by heating the chemical reactants further only.

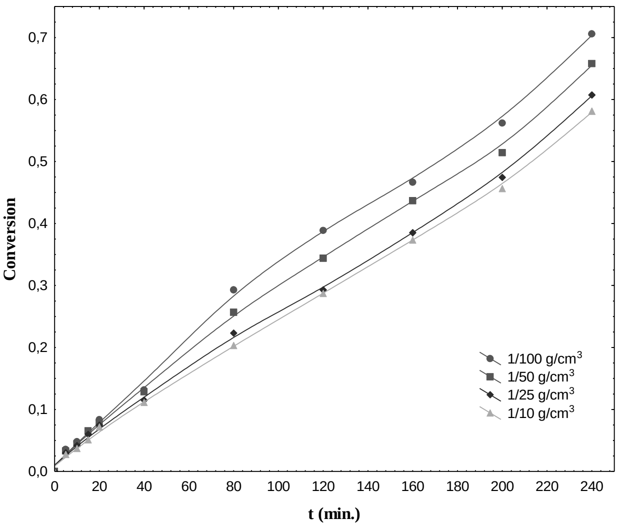

Figure 4. Change graph between time and conversion for different solid-liquid ratios.

3.2.2. Effect of S/L ratio

Changes in the solid / liquid (S / L) ratio allow the observation of the dissolution kinetics of chalcopyrite, such as 1/100, 1/50, 1/25 and 1/10 g cm^{-3}, respectively. The dissolution curves are demonstrated in Figure 4. As shown in Figure 4, the dissolution rate changes in reverse with the S / L ratio. The decrease in dissolution rate with increasing solids can be explained by the decrease in the number of chalcopyrite particles per the amount of solution. If the reaction mixture has high solid-to-liquid ratio, the slurry becomes viscous and hampers ion mobility, hence decreasing the leaching efficiency.[7]

3.2.3. Effect of stirring speed

As can be seen from the reactions 3 and 4, the leaching of chalcopyrite is a heterogeneous reaction. This involves mass transfer of the reactants on the chalcopyrite surface.[8] The effect of the stirring speed on the dissolution rate of chalcopyrite was investigated at 300, 500, 700 and 900 rpm. The change between stirring speed and conversion are shown in Figure 5. It can be seen from Figure 5 that the effect of stirring speed is very small.[9]

3.2.4. Effect of particle size

After fragmentation, four fractions such as -50 + 70, -70 + 100, -100 + 120, and -120 + 140 µm were eliminated. According to the dissolution curves presented in Figure 6, a direct correlation formed between the magnitude of mineral particles and the dissolution rate because the smaller parts have more surface area and less volume.

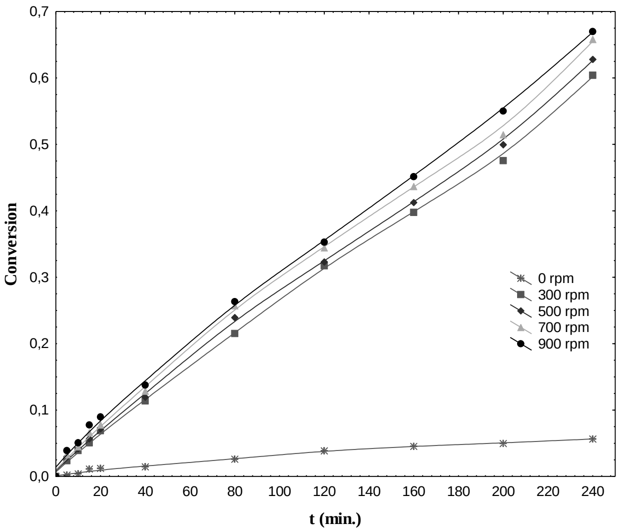

Figure 5. Change graph between time and conversion for different stirring speeds.

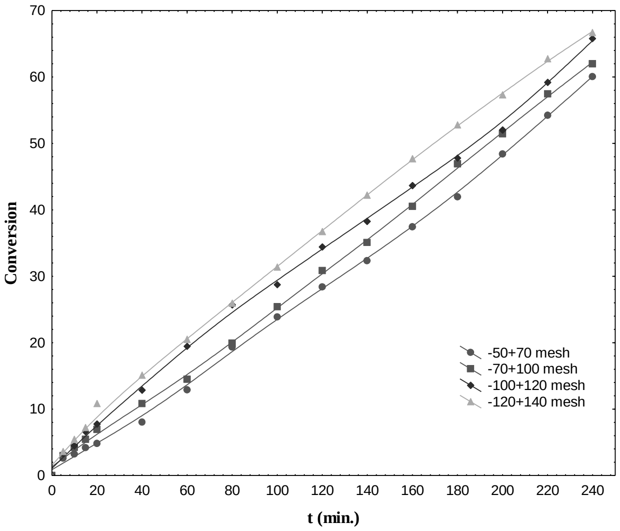

Figure 6. Change graph between time and conversion for different particle sizes.

The high ratio of surface area to volume means that the leaching has more opportunity to contact with the mineral.[10]

3.2.5. Effect of H_2SO_4 concentration

In this study, the reagent for the leaching reaction was sulphuric acid. The H_2SO_4 concentration needs to be raised up to a specific value and not beyond that for leaching efficiency. In response to variations of 2.0, 3.0, 4.0 and 5.0 mol dm^{-3}, dissolution curves were plotted. The graph can be seen in Figure 7. It was determined that the level of dissolution of the process increased with the increase in the concentration of the sulfuric acid solution. The efficient dissolution reaction is associated with higher H_2SO_4 concentrations.[11]

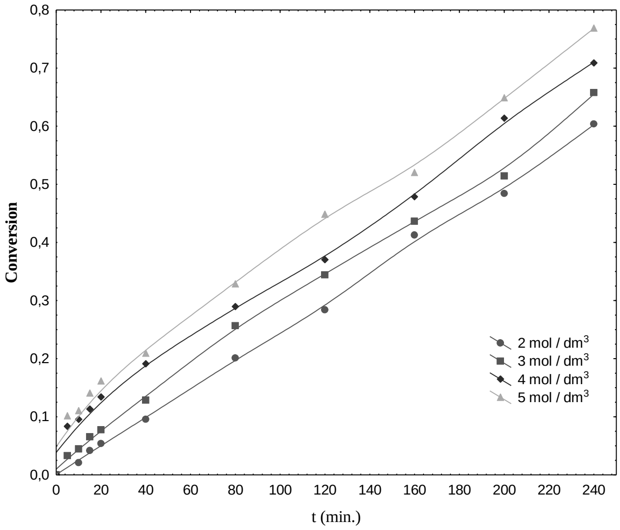

Figure 7. Change graph between time and conversion for different concentrations of H_2SO_4.

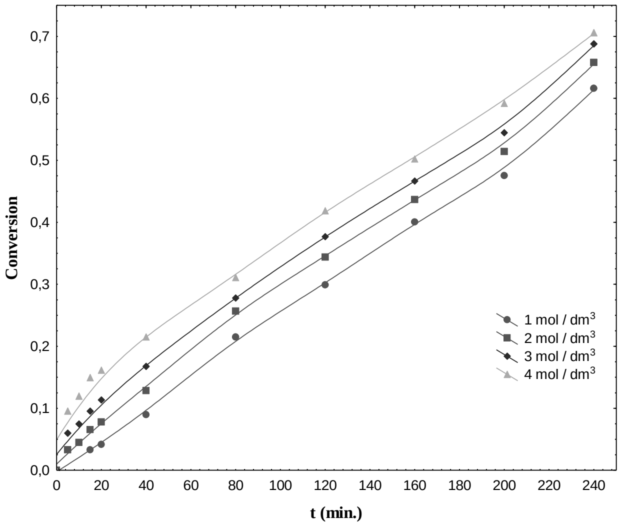

Figure 8. Change graph between time and conversion for different concentration of KNO_3.

3.2.6. Effect of KNO_3 concentration

Potassium nitrate is both a crystalline salt and a strong oxidizer, and it is used especially in gunpowder, fertilizer and medicine. The effect of the $KN0_3$ concentration on the leaching grade was determined at a $KN0_3$ concentration between 1.0 and 4.0 mol dm^{-3} and at a time interval of 3 to 240 minutes. The dissolution curves are given in Figure 8. From Figure 8, the level of dissolution of the process increases with an increase in the concentration of potassium nitrate solution.[21] Because of the fact that sulphuric acid without oxidants does not react with chalcopyrite, the reaction rate increases with an increase in KNO_3 concentration. The oxidation potential of nitrate ions increases the acidity of the solution. Therefore, this situation increases the leaching rate.[3]

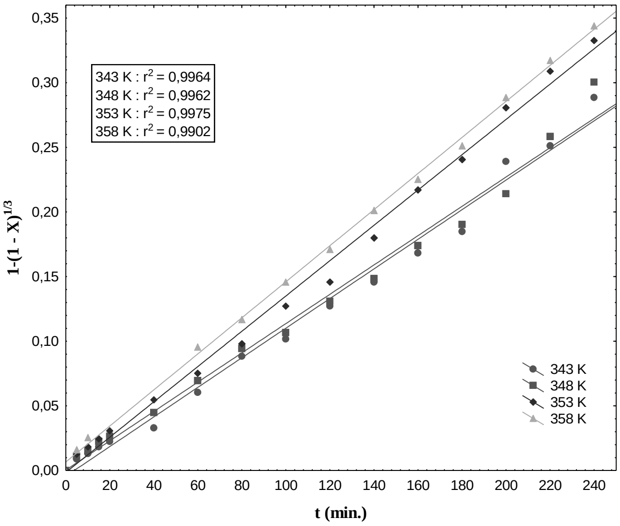

Figure 9. Change between 1-(1-X)$^{1/3}$ and t for different reaction temperature.

3.2.7. Kinetics analysis

In order to determine the kinetic parameters and the reaction rate control step of the dissolution reaction between chalcopyrite mineral and sulphuric acid with potassium nitrate solutions, non-catalytic heterogeneous reaction models were applied on experimental data.[12] Heterogeneous reaction model can be used to study the heterogeneous reaction process between solid and liquid. The non-reacting shrinking core model was applied to analyse the trial results and to make an assessment of the speed-limiting step.[13] Rate equations can be obtained from the heterogeneous reaction model, especially for each control mechanism. The heterogeneous reaction model is numerically and analytically used for solid-liquid heterogeneous systems. The integral ratio equations for the non-reacted shrink core model and other models are presented in Table 4. Following the experiments, the analysis of the results was performed as best practice using the above-mentioned models to evaluate the kinetics of the leaching process. When the film diffusion is much quicker than the chemical reaction, the leaching action refers to the controlled chemical reaction. Also, the regression coefficients of models calculated in the study can be reviewed in Table 4. As a result of the regression analysis, the results of the experiment were found to be in accordance with Eq. (6) in Table 4. Therefore, it can be said that this reaction is controlled by chemical reaction. Starting from this, the leaching process is limited by the chemical reaction. The

DOI: http://dx.doi.org/10.32571/ijct.515611 **E-ISSN:2602-277X**

Table 4. Integral rate equations for non-reactive shrink core model and other models

Rate-controlling step	Rate equation		r^2	Equation
Chemical reaction	$t/t^* = [1-(1-X_B)^{1/3}]$	$t^* = \rho_B R / bksC_{Ag}$	0.998	(5)
Film diffusion control	$t/t^* = X_B$	$t^* = \rho_B R / 3bkC_{Ag}$	0.961	(6)
Diffusion control through the ash or product layer	$t/t^* = [1-3(1-X_B)^{2/3} + 2(1-X_B)]$	$t^* = \rho_B R^2 / 6bDeC_{Ag}$	0.941	(7)
First-order pseudo-homogeneous model		$-\ln(1-X) = kt$	0.925	(8)
Second-order pseudo-homogeneous model		$(1-X)^{-1} = kt$	0.912	(9)
Avrami model		$-\ln(1-X) = kt^m$	0.933	(10)

t*: Reactionary time for full conversion, min.

regression coefficient of the model was calculated as 0.998. This is a fairly high value. For different reaction temperatures, a graph between time and 1- $(1-X)^{1/3}$ can be seen in Figure 9.

In reactions controlled by the chemical reaction, reactionary time for full conversion (t*) is proportional to the starting radius of a solid particle (R).[14-18] The t* values versus R were plotted. The high linearity between t* and R can be seen in Figure 10. The regression coefficient (r^2) between t* and R was found to be 0.9965. In diffusion controlled reaction, reactionary time for full conversion (t*) is proportional to square of the starting radius of a solid particle (R^2). The regression coefficient (r^2) between t* and R^2 was determined to be 0.9566. This situation confirms that rate controlling step for this process is governed by the chemical reaction model. The value of the activation energy helps to estimate the speed control step. In order to find the activation energy of the reaction, Arrhenius graphs between *ln k* and *1/T* must be plotted. For this reason, the obtained graph can be seen in Figure 11. The correlation coefficient of this graph is 0.9801. The slopes of the straight line give the activation energy of the reaction. The activation energy was found to be 78.25 kJ mol^{-1}. The temperature dependence of diffusion controlled processes is low. The temperature dependence of chemical reaction controlled processes is very high. In diffusion controlled processes, the activation energy varies between about 4 and 12 kJ mol^{-1}.[12] The activation energy of the leaching process controlled by the surface chemical reactions was observed to be more than 40 kJ mol^{-1}.[19] There is matching evidence in literature.[13,20] Furthermore, this energy level confirms that the dissolution rate for chalcopyrite is measured under the control of a chemical reaction.

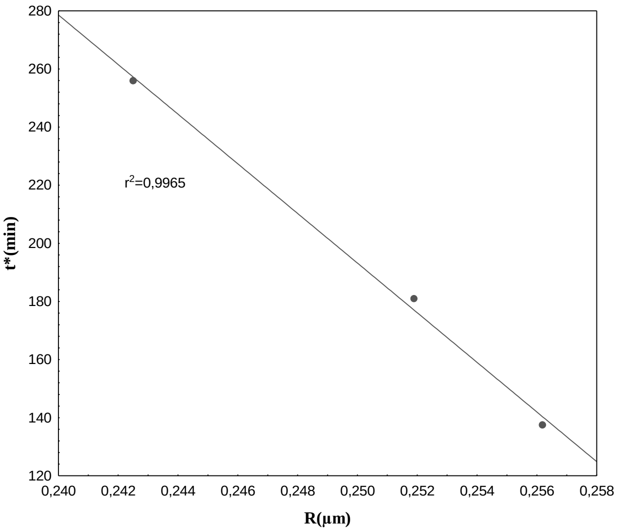

Figure 10. Linearity change between t^* and R.

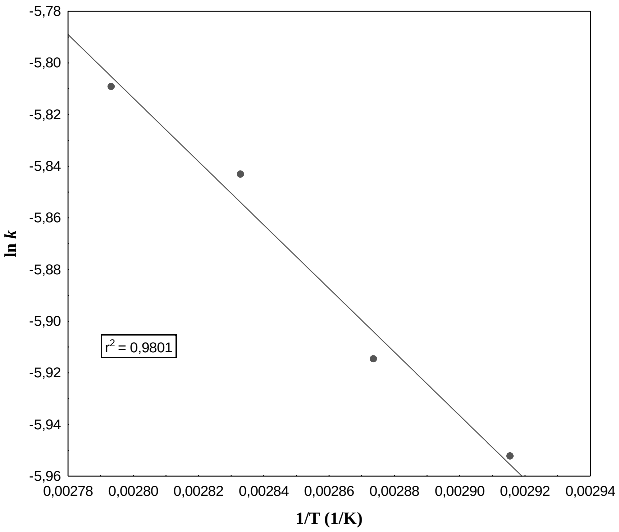

Figure 11. Arrhenius graph.

4. CONCLUSIONS

The dissolution kinetics of chalcopyrite with potassium nitrate in sulphuric acid solutions with the help of a mechanical agitation system was investigated in the work. As process parameters, temperature, S/L ratio, stirring speed, particle size, concentration of sulphuric acid and potassium nitrate solutions were selected.

As a result of the study, it may be concluded that:

- Rate controlling step for this process is the chemical reaction model.
- The activation energy was found to be 78.25 kJ mol^{-1}.
- The higher reaction temperature and smaller S/L ratio has a slight effect on dissolution rate.
- The oxidation potential of nitrate ions increases the acidity of the solution.
- KNO_3 in H_2SO_4 solution can be used for the dissolution of chalcopyrite.

Nomenclature

b	Stoichiometric coefficient
C	Concentration of KNO_3 solution, mol m^{-3}
C_{Ag}	Concentration of a in the bulk solution, mol m^{-3}
D	Mean particle size, m
D_e	Diffusion coefficient, m^2 min^{-1}
E_A	Activation energy, J mol^{-1}
k_d	Mass transfer coefficient, m min^{-1}
k_s	Reaction rate constant for surface reaction, mol min^{-1}
k_o	Frequency or pre-exponential factor, $min.^{-1}$
L	Amount of liquid, dm^3
n	Mol number, mol
r	Correlation coefficient
R	Universal gas constant, J mol^{-1} K^{-1}
R	Initial radius of a particulate solid, m
S	Amount of solid, g
T	Reaction temperature, K
t	Reactionary time, min.
t*	Reactionary time for full conversion, min.
X	Fractional conversion of chalcopyrite
W	Stirring speed, rpm
ρ_B	Molar density of solid reactant, mol m^{-3}

Conflict of interests

Authors declare that there is no a conflict of interest with any person, institute, company, etc.

REFERENCES

1. Dimitrijevic, M.; Antonijevic, M.; Jankovic, Z., *Hydrometallurgy* **1996,** 42 (3), 377-386.

2. Dutrizac, J. E., *Metall. Trans. B* **1978,** *9 (3)*, 431-439.

3. Vračar, R. Ž.; Vučković, N.; Kamberović, Ž., *Hydrometallurgy* **2003,** 70 (1-3), 143-151.

4. Nemodruk, A. A.; Karalova, Z. K., *Analytical Chemistry of Boron*, Israel Program for Scientific Translations, 1965.

5. Sookg, D.; West, D.; Holler, F., *Saunders College Publishing* **1996**.

6. Naderi, H.; Abdollahy, M.; Mostoufi, N.; Koleini, M.; Shojaosadati, S.; Manafi, Z., *Int. J. Min. Met. Mater.* **2011,** 18 (6), 638-645.

7. Panda, L.; Rao, D.; Mishra, B.; Das, B., *Miner. Metall. Proc.* **2014,** 31 (1), 57-65.

8. Papangelakis, V.; Demopoulos, G., *Hydrometallurgy* **1991,** 26 (3), 309-325.

9. Kurtbas, A.; Kocakerim, M. M.; Küçük, Ö.; Yartasi, A., *Ind. Eng. Chem. Res.* **2006,** 45 (6), 1857-1862.

10. Levenspiel, O., *Wiley-Eastern Limited, New York* **1972**.

11. Aydogan, S.; Ucar, G.; Canbazoglu, M., *Hydrometallurgy* **2006,** 81 (1), 45-51.

12. Demirkıran, N., *Hydrometallurgy* **2009,** 95 (3-4), 198-202.

13 Alkan, M.; Doğan, M.; Namli, H., *Ind. Eng. Chem. Res.* **2004,** 43 (7), 1591-1598.

14. Habashi, F., *Kinetics of metallurgical processes*. 1999.

15. Dönmez, B.; Demir, F.; Laçin, O., J. Ind. Eng. Chem. **2009,** 15 (6), 865-869.

16. Kuşlu, S.; Dişli, F. Ç.; Çolak, *J. Ind. Eng. Chem.* **2010,** 16 (5), 673-678.

17. Guliyev, R.; Kuşlu, S.; Çalban, T.; Çolak, S., *J. Ind. Eng. Chem.* **2012,** 18 (4), 1202-1207.

18. Guliyev, R.; Kuşlu, S.; Çalban, T.; Çolak, S., *J. Ind. Eng. Chem.* **2012,** 18 (1), 38-44.

19. Jackson, E., *Hydrometallurgical extraction and reclamation*. Chichester: Horwood; New York, Wiley: 1986.

20. Yartasi, A.; Ozmetin, C.; Kocakerim, M.; Demirhan, M., *Chim. Acta TUR.* **1998,** 26 (2), 7-14.

DOI: http://dx.doi.org/10.32571/ijct.515611 **E-ISSN:2602-277X**

21. Çolak, S.; Alkan, M.; Kocakerim, M. M., *Hydrometallurgy* **1987,** 18 (2), 183-193.

22. Antonijević, M.; Janković, Z.; Dimitrijević, M., *Hydrometallurgy* **1994,** 35 (2), 187-201.

23. Antonijević, M.; Janković, Z.; Dimitrijević, M., *Hydrometallurgy* **2004,** 71 (3), 329-334.

24. Ikiz, D.; Gülfen, M.; Aydın, A., *Minerals engineering* **2006,** 19 (9), 972-974.

25. Al-Harahsheh, M.; Kingman, S.; Al-Harahsheh, A., *Hydrometallurgy* **2008,** *91* (1), 89-97.

26. Sokić, M. D.; Marković, B.; Živković, D., *Hydrometallurgy* **2009,** *95* (3), 273-279.

27. Xian, Y.; Wen, S.; Deng, J.; Liu, J.; Nie, Q., *Can. Metall. Quart.* **2012,** 51 (2), 133-140.

ORCID

https://orcid.org/0000-0001-6302-5107 (H. Dikme)

https://orcid.org/0000-0003-4830-5949 (S. Kuşlu)

https://orcid.org/0000-0003-0431-1861 (Ö. Karagöz)